applied sciences

MDPI

Article

Optical Study of Electronic Structure and Photoinduced Dynamics in the Organic Alloy System $[(EDO\text{-}TTF)_{0.89}(MeEDO\text{-}TTF)_{0.11}]_2PF_6$

Tadahiko Ishikawa [1,*], Yohei Urasawa [1], Taiki Shindo [1], Yoichi Okimoto [1], Shin-ya Koshihara [1,2], Seiichi Tanaka [1], Ken Onda [3], Takaaki Hiramatsu [4], Yoshiaki Nakano [4,5], Koichiro Tanaka [6] and Hideki Yamochi [4,5]

1 Department of Chemistry, School of Science, Tokyo Institute of Technology, 2-12-1, Oh-okayama, Meguro-ku, Tokyo 152-8551, Japan; urasawa.yoyo.yuyu@gmail.com (Y.U.); rs_co2toosa9@hotmail.co.jp (T.S.); okimoto.y.aa@m.titech.ac.jp (Y.O.); skoshi@cms.titech.ac.jp (S.-y.K.); eagle00sp2@sepia.plala.or.jp (S.T.)
2 Institute of Innovative Research, Tokyo Institute of Technology, 2-12-1, Oh-okayama, Meguro-ku, Tokyo 152-8551, Japan
3 Department of Chemistry, Kyushu University, 744, Motooka, Nishi-ku, Fukuoka, Fukuoka 819-0395, Japan; konda@chem.kyushu-univ.jp
4 Research Center for Low Temperature and Materials Sciences, Kyoto University, Sakyo-ku, Kyoto 606-8501, Japan; hi-taka@kch.biglobe.ne.jp (T.H.); nakano@kuchem.kyoto-u.ac.jp (Y.N.); yamochi@kuchem.kyoto-u.ac.jp (H.Y.)
5 Division of Chemistry, Graduate School of Science, Kyoto University, Sakyo-ku, Kyoto 606-8502, Japan
6 Department of Physics, Graduate School of Science, Kyoto University, Sakyo-ku, Kyoto 606-8502, Japan; kochan@scphys.kyoto-u.ac.jp
* Correspondence: tishi@chem.titech.ac.jp; Tel.: +81-3-5734-2614

Received: 28 January 2019; Accepted: 15 March 2019; Published: 20 March 2019

Featured Application: Ultra-fast optical communication, optical memory, photo-switch.

Abstract: Over the past two decades $(EDO\text{-}TTF)_2PF_6$ (EDO-TTF = 4,5-ethylenedioxytetrathiafulvalene), which exhibits a metal–insulator (M–I) phase transition with charge–ordering (CO), has been investigated energetically because of attractive characteristics that include ultrafast and massive photoinduced spectral and structural changes. In contrast, while its crystal structure has much in common with the $(EDO\text{-}TTF)_2PF_6$ crystal, the organic alloy system of $[(EDO\text{-}TTF)_{0.89}(MeEDO\text{-}TTF)_{0.11}]_2PF_6$ (MeEDO-TTF = 4,5-ethylenedioxy-4′-methyltetrathiafulvalene) exhibits a quite different type of M–I phase transition that is attributed to Peierls instability. Here, an optical study of the static absorption spectra and the time-resolved changes in the absorption spectra of $[(EDO\text{-}TTF)_{0.89}(MeEDO\text{-}TTF)_{0.11}]_2PF_6$ are reported. The observed absorption spectra related to the electronic structure are highly anisotropic. With a reduction in temperature (T), the opening of a small optical gap and a small shift in the center frequency of the C=C stretching mode are observed along with the M–I phase transition. Additionally, photoinduced transient states have been assigned based on their relaxation processes and transient intramolecular vibrational spectra. Reflecting small valence and structural changes and weak donor–anion interactions, a photoinduced transient state that is similar to the thermal-equilibrium high-T metallic phase appears more rapidly in the alloy system than that in $(EDO\text{-}TTF)_2PF_6$.

Keywords: photoinduced dynamics; metal–insulator transition; charge ordering; 1/4-filled band system; $2k_F$ modulation; electron correlation; electron–lattice interaction; electron molecular interaction; donor–anion interaction; organic alloy

1. Introduction

Photoinduced phenomena are popular research topics, not only in the solid-state physics field but also in general science for basic and applied fields. Photoinduced phenomena related to the phase transition in the solid-state contribute to the development of new photofunctional materials that can be used to realize high-speed and large-scale data communication, computing, and memory applications [1,2]. Among the various solid-state materials that are available, the molecular crystal system with a 1/4-filled band and a quasi-one-dimensional electronic structure [3–7] is regarded as the most popular target system for the study of ultrafast photoinduced dynamics because of its intrinsically strong electron–electron and electron–phonon correlated nature, which governs the dynamics in the time-scale of the ps order.

In particular, $(EDO\text{-}TTF)_2PF_6$ (EDO-TTF = 4,5-ethylenedioxytetrathiafulvalene), which exhibits a metal–insulator (M–I) phase transition with changes in temperature (T), has been investigated energetically because of its unique insulating phase: its $2k_F$ (k_F: Fermi wavenumber) charge and lattice modulation with large amplitude that are attributed to its charge–ordering (CO) phase, with a charge pattern of (0110) [7–12]. The origin that causes the characteristic low-T insulating phase has been studied both experimentally and theoretically, however, it remains under discussion. In addition to the unique electronic structure, the ultrafast optical and structural changes after irradiation by fs laser pulses have also been reported [13–18]. From the analysis of transient reflectivity, $(EDO\text{-}TTF)_2PF_6$ shows a temporal CO with the charge pattern of (1010), which is different from that of low-T phase and observed only immediately after photoexcitation [14]. The cooperation/competition of several types of interactions, including electron–electron, electron–lattice, and donor–anion interactions, must be regarded as important factors for realization of the unique low-T insulating phase of $(EDO\text{-}TTF)_2PF_6$ and its photoinduced dynamics. Therefore, a comparative study of photoinduced dynamics in similar classes of materials with different physical parameter values is essential to understanding of the roles of these interactions in each material's photo-response [19–21]. Here we present the first report of a study on the dynamics of the photoinduced phase transition process in the organic alloy system $[(EDO\text{-}TTF)_{0.89}(MeEDO\text{-}TTF)_{0.11}]_2PF_6$ (MeEDO-TTF = 4,5-ethylenedioxy-4′-methyltetrathiafulvalene), which shows a quite different class of M–I phase transition than that of $(EDO\text{-}TTF)_2PF_6$ despite the similarity of crystal structure in high-T metallic phase.

The organic alloy system $[(EDO\text{-}TTF)_{1-x}(MeEDO\text{-}TTF)_x]_2PF_6$ has been developed recently and its M–I phase transition has been reported [22,23]. A comparison of the chemical structures of the EDO-TTF and MeEDO-TTF molecules is depicted in Figure 1. Obviously, the MeEDO-TTF molecule is larger than the EDO-TTF molecule. The crystal structure of the organic alloy system for values of x of less than 0.48 is observed to be analogous to that of the $(EDO\text{-}TTF)_2PF_6$ structure. A phase diagram of this system in the T and x planes in which two types of M–I phase transition are involved has been reported previously [22,23]. At approximately $x = 0$, the first type of M–I phase transition is observed to be a CO-type transition, which was reported for $(EDO\text{-}TTF)_2PF_6$ [8–10]. However, the second M–I phase transition type is witnessed over an adequate range of x ($0.09 \leq x \leq 0.21$). In the low-T insulating phase of the second type of M–I phase transition, clear charge disproportionation was not observed, but the appearance of a Peierls-like structural modulation was confirmed [22,23]. In the $x < 0.48$ range, a metallic phase structure is quite common, although there is a slight increase in the distance between the donor and the anion due to the substitution of the donor molecule from EDO-TTF to MeEDO-TTF. From these results, it has been proposed that the extension of the distance between the donor and the anion can modulate the donor–anion interaction, which then determines whether the first or second type of the M–I phase transition occurs in this class of materials [22]. Hereafter, the first type of M–I phase transition is called the CO-type M–I phase transition, while the second type is called the Peierls-type M–I phase transition. A photoinduced I-to-M phase transition in the I phase, which occurs alongside the Peierls-type M–I transition system, is an attractive topic for clarification of the role of the donor–anion interaction during photoinduced dynamics.

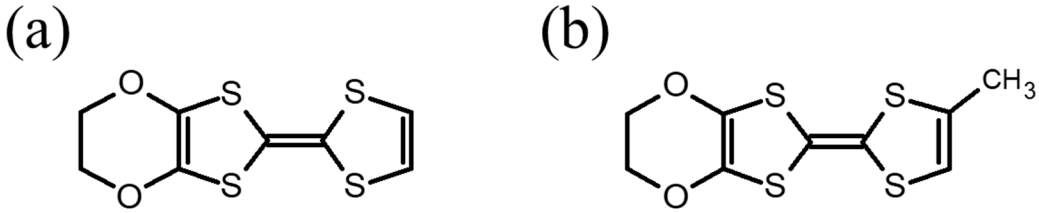

Figure 1. Chemical structures of (**a**) EDO-TTF and (**b**) MeEDO-TTF molecules.

2. Materials and Methods

$[(EDO\text{-}TTF)_{0.89}(MeEDO\text{-}TTF)_{0.11}]_2PF_6$ single crystals were grown for this study using a method that has been described previously in the literature [22]. The resulting crystals show the Peierls-type M–I phase transition. The needle-shaped crystals obtained had a mirror-like flat surface that lay parallel to the molecular-stacking axis (the crystal structure is shown in [22]). Due to the extremely brittle nature of the crystal around the M–I transition temperature (T_c), electrical resistivity measurements resulted in a resistance jump due to the crystal cracking at 210 K. Based on the T dependences of the optical spectra (see below), T_c was deduced to be between 150 and 200 K, which is consistent with the available structural data for alloys containing higher and lower numbers of MeEDO-TTF molecules [23].

We microtomed the crystals to a thickness of 300 nm in the direction parallel to the mirror-like surface. These microtomed thin crystals were mounted on the transmission electron microscopy (TEM) grids made from copper with a 400 mesh size.

The transmission spectra at room temperature (RT) were measured at the mid-infrared (mid-IR: 0.08–1.0 eV) and near-IR to visible (0.9–2.0 eV) ranges with Fourier-type and diffraction-grating-type monochromators, respectively. The incident light was linearly polarized along the stacking axis of the donor molecules (denoted by $E \parallel$ stack) or perpendicular to the same axis (denoted by $E \perp$ stack). We measured the T dependence of the transmission spectra at between 0.08 and 0.8 eV. The TEM grid was attached onto the copper plate using conductive silver paste to ensure good thermal contact with the sample holder in a conduction-type cryostat.

We observed an ultrafast transmission change occurring at 0.27 eV via conventional pump–probe-type time-resolved transmission measurements. The laser pulses from a Ti:sapphire regenerative amplifier (pulse duration: 120 fs; photon energy: 1.56 eV; and repetition rate: 1 kHz) were utilized as the light source of pump light. The probe light with photon energy of 0.27 eV was generated by using an optical parametric amplifier (OPA) and the optical difference-frequency generation (DFG) process from the 1.56 eV pulsed light. Additionally, the spot diameters of the pump and probe light were adjusted to be approximately 350 μm and within 50 μm, respectively. We modulated the pump pulse train at 500 Hz using an optical chopper and recorded the difference between the intensities of the transmitted probe pulse with and without photoexcitation to achieve a higher signal-to-noise ratio. The time delay between the pump light and the probe light was controlled by using the translational stage which provides the optical path length difference.

The experimental setup used to perform time-resolved IR vibrational spectroscopy was similar to that reported in previously conducted studies [24–26]. The broadband mid-IR probe-pulse (pulse duration: 120 fs, centered around 1580 cm^{-1}; spectral width: 150 cm^{-1}) was generated using the OPA and the DFG process from the output of a femtosecond Ti:sapphire regenerative amplifier. We detected the probe pulse that was transmitted from the sample using a 64-channel linear HgCdTe (MCT) detector array through a 19-cm-long polychromator. During the measurements, the sample was fixed in the sample holder in a conduction-type cryostat with a refrigerator.

3. Results

3.1. Anisotropy of the Electronic Structure of [(EDO-TTF)$_{0.89}$(MeEDO-TTF)$_{0.11}$]$_2$PF$_6$

The transmission spectra obtained using linearly polarized light were converted into optical density (OD) spectra, which are related to the optical absorption spectra. The anisotropy of the OD spectra of [(EDO-TTF)$_{0.89}$(MeEDO-TTF)$_{0.11}$]$_2$PF$_6$ at RT is depicted in Figure 2. In the figure the presence of spiky structures in the energy range below 0.25 eV can be attributed to intramolecular vibrations, which are discussed in the next subsection. It is observed that the characteristic features of the OD spectra are similar to those of the optical conductivity spectra of (EDO-TTF)$_2$PF$_6$; these peaks can thus be assigned to those arise from the same origins [9]. The absorption peaks at approximately 1.8 eV can be attributed to the intra-molecular electron transition that occurs in EDO-TTF or MeEDO-TTF cation radicals. The anisotropy in the energy range below 1.5 eV is clearly illustrated by these spectra. In this energy range, the E ∥ stack spectrum exhibited an intense and broad peak, however, the OD for E ⊥ stack spectrum was rather weak. This energy range is lower than that for intramolecular electronic transition. It is naturally expected that the electronic structure of the title material will be anisotropic because of the strong hybridizations of the molecular orbital along the molecular stacking direction, similar to (EDO-TTF)$_2$PF$_6$. The observed anisotropic and strong absorption band for the energy range below 1.5 eV can, thus, be assigned to the charge transfer excitation between the nearest neighbor donor sites.

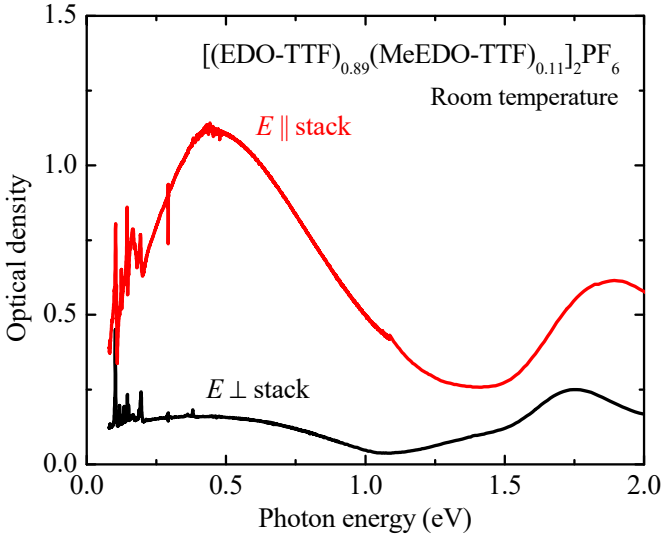

Figure 2. Optical-density spectra of thin crystals (thickness of approximately 300 nm) of [(EDO-TTF)$_{0.89}$(MeEDO-TTF)$_{0.11}$]$_2$PF$_6$ with E ∥ stack (red line) and E ⊥ stack (black line) polarizations at room temperature (RT).

3.2. M–I Phase Transition Observed in the OD Spectra of [(EDO-TTF)$_{0.89}$(MeEDO-TTF)$_{0.11}$]$_2$PF$_6$

The T dependence of the OD spectra was measured to detect the changes in the electronic or molecular structures caused by the M–I phase transition reported previously [22]. Unfortunately, no clear spectral changes could be observed in the E ∥ stack OD spectra down to the lowest T value used in this study, i.e., 70 K. Contrary, the E ⊥ stack spectra showed a significant T dependence and is discussed in this study. As already shown in Figure 2, the E ⊥ stack OD spectrum at RT (in the high-T metallic phase) shows weak but finite absorption in the mid-IR range below 1 eV. The change in the spectral shape of the E ⊥ stack OD is depicted in Figure 3a as a function of decreasing T. At 280 K, the OD spectrum for the energy range below 0.3 eV was observed to be almost flat, with the exception of the very sharp peaks caused by the intramolecular vibrational modes below 0.2 eV. The intensity of the E ⊥ stack OD gradually increased as T decreased from RT to T_c; specifically, a new

absorption band centered at approximately 0.2 eV appeared below T_c. The presence of an optical gap structure is indicated by the OD spectrum shape at 70 K. The value of the energy gap was estimated to be approximately 0.05 eV by extrapolation of the measured OD spectrum, as indicated by the dashed line in Figure 3a. The gradual change in the spectral shape and the small energy gap value appeared to be consistent with the gradual M–I phase transition and the small T dependence of the resistivity in the low-T insulating phase that was reported in [22].

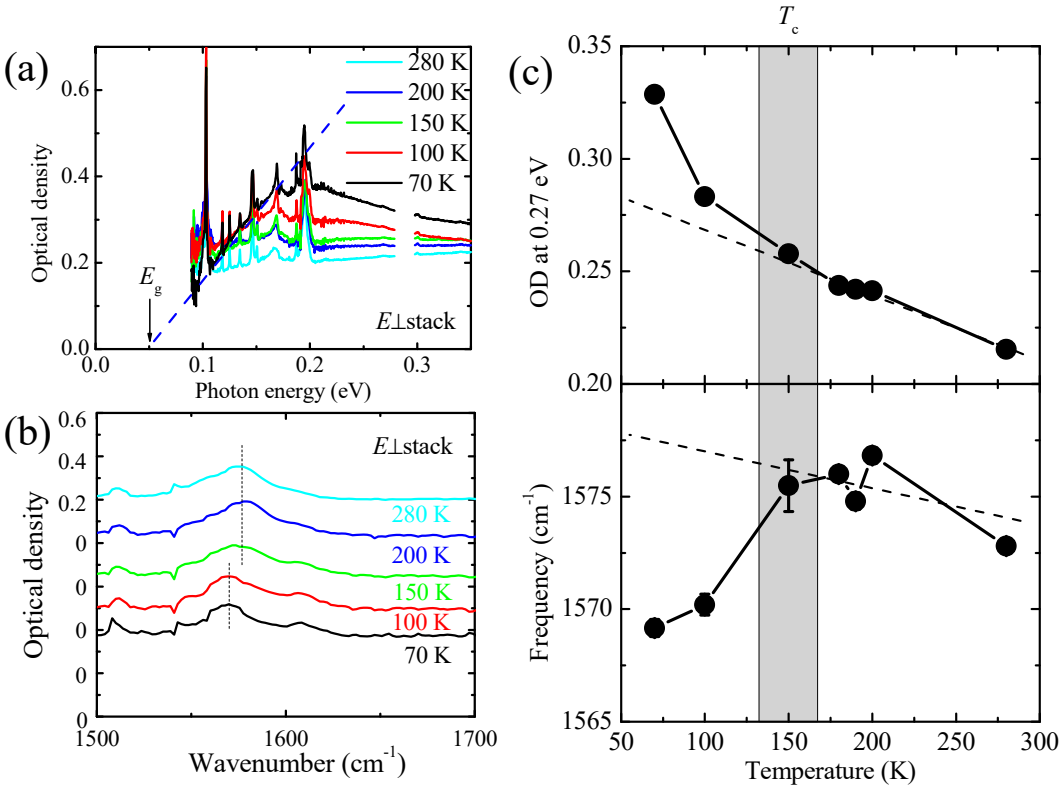

Figure 3. (**a**) Temperature (T) dependence of the optical density (OD) spectra with $E \perp$ stack polarization. The dashed line in this figure is a simple extrapolation of the low-energy structure of the observed OD spectrum. (**b**) Magnified OD spectra in the energy range around the C=C stretching mode in EDO-TTF (or MeEDO-TTF) molecules. (**c**) Upper panel: the OD value at 0.27 eV. Lower panel: center frequency of the C=C stretching mode. The shaded region represents the T range in which the resistivity change due to the M–I phase transition has been reported [22]. The dashed lines in the upper and lower panel indicate the extrapolation of the T dependence in the high-T metallic phase.

The T dependence of the OD value at 0.27 eV is depicted in the upper panel of Figure 3c. The OD value increases uniformly as the sample is cooled in the T range above T_c. However, when the sample is cooled down below T_c, it deviates from the extrapolated T dependence in the high-T range, as indicated by the dashed line below T_c. From these results, it is reasonable to propose that the OD value at 0.27 eV strongly reflects the formation of the optical gap accompanied by the M–I transition and this can act as a good probe for photo-modulation of the electronic structure, i.e., the appearance/disappearance of the optical gap.

Another spectral change related to the intramolecular vibration was also observed to be accompanied by the M–I phase transition in this system. The magnified OD spectrum is shown in Figure 3b. The absorption peak of the C=C stretching mode of the EDO-TTF (or MeEDO-TTF) molecules was located at approximately 1575 cm^{-1} at 280 K ($T > T_c$). The center frequency of this vibrational mode (as indicated by the vertical dashed lines in Figure 3b) was shifted to a lower frequency by reducing T across T_c. The peak positions of this mode at each T value are plotted in the

lower panel of Figure 3c. This frequency shift reflects the small structural change in the EDO-TTF (or MeEDO-TTF) molecules when accompanied by the M–I phase transition.

3.3. Photoinduced Dynamics in the Low-T Insulating Phase Observed via Pump-Probe Time-Resolved Transmission Spectroscopy in the Mid-IR Range

Pump–probe type time-resolved transmission spectroscopy was performed in the mid-IR range on the low-*T* insulating phase of the organic alloy system. The temporal dependence of the photoinduced OD change (ΔOD) at 0.27 eV, which is designated as a good probe for gap formation, as discussed in the previous subsection, is shown in Figure 4. The excitation photon energy of 1.56 eV is the fundamental photon energy of our regenerative amplifier systems, which ensured good laser fluence stability. The photoexcitation corresponded to excite the intramolecular electronic transition. The excitation fluence was observed to be approximately 7.00×10^{15} photons/cm^2. A rapid decrease in the OD value was observed just after the photoexcitation followed by the relaxation processes to recover the OD. The observed negative ΔOD value indicates the photoexcitation-induced collapse of the electronic gap structure. The relaxation processes can be assigned to the partial recovery of the electronic gap structure.

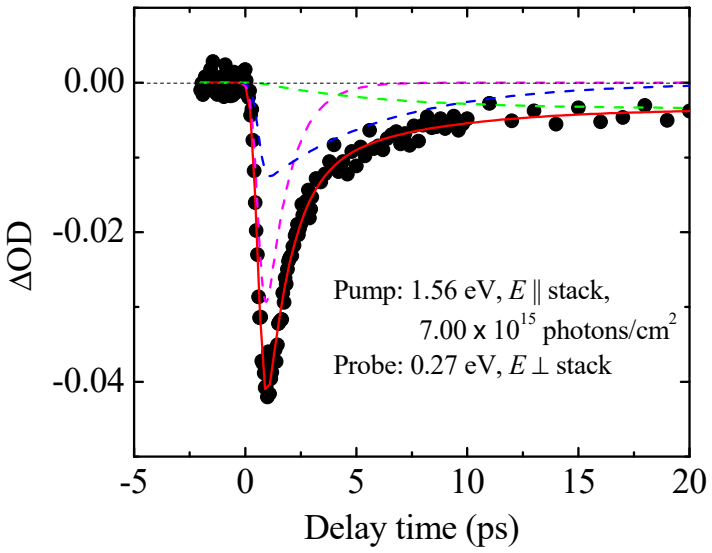

Figure 4. Temporal dependence of the photoinduced OD change (ΔOD) at 70 K (closed black circles). The excitation conditions are 1.56 eV, E | | stack polarization, and 7.00×10^{15} photons/cm^2. The probe photon energy is 0.27 eV with the $E \perp$ stack polarization direction. The thin red line indicates the results of the fitting analysis using function (1). The pink, blue, and green dashed lines represent the temporal dependences of each component of fitting function (1).

To determine the photoinduced processes that are involved, a fitting analysis was performed using the following function:

$$f(t) = \begin{cases} A\exp\left(-\frac{t-t_0}{\tau_1}\right) + B\exp\left(-\frac{t-t_0}{\tau_2}\right) + C\left[1-\exp\left(-\frac{t-t_0}{\tau_2}\right)\right], & (t \geq t_0) \\ 0, & (t < t_0) \end{cases} . \quad (1)$$

Here, the amplitudes of the terms are denoted by A, B, and C. The relaxation time constants are denoted by τ_1 and τ_2. Furthermore, the delay time and the time-zero point are denoted by t and t_0, respectively. The three terms in Equation (1) correspond to the three types of relaxation processes from the photoinduced transient states to the ground states. The first and second terms have relaxation constants of τ_1 and τ_2, respectively. The third term represents the relaxation process for which the time scale is over the delay time range shown in Figure 4. To perform the fitting analysis, the finite

durations of the pump and probe pulses were considered by calculating the convolution using a time-dependent Gaussian-type function. The width of this Gaussian-type function was introduced as a fitting parameter and the estimated value corresponded with the laser pulse width (120 fs). The results of the fitting analysis of the experimental data and the first, second, and third terms in Equation (1) are depicted in Figure 4. From the analysis, the best fitting parameters for τ_1 and τ_2 were estimated to be 1.1 $\pm$ 0.1 and 5.6 $\pm$ 3.2 ps, respectively. When t_0 is set at 0 ps, the simulated curve with the above mentioned fitting parameters reproduces the experimental curve quite well.

3.4. Photoinduced Dynamics in the Low-T Insulating Phase Observed via Pump-Probe Time-Resolved Vibrational Spectroscopy in the Energy Range of the Intramolecular Vibration Modes

Pump–probe type time-resolved vibrational spectroscopy was performed at 100 K in the low-*T* insulating phase in transmission mode to study the photoinduced dynamics from a structural viewpoint. The excitation conditions were almost the same as those used in the previous subsection, except for a slightly higher fluence of 3.49 $\times$ 10^{16} photons/cm^2. The C=C stretching mode of the EDO-TTF (or MeEDO-TTF) molecules can act as a good probe for the molecular structural change accompanied by the M–I phase transition, as discussed earlier in Section 3.2. Therefore, the center wavenumber for this measurement was set at approximately the center frequency of the C=C stretching mode. The temporal dependence of the ΔOD signal at several probe light wavenumbers is shown in Figure 5. The temporal dependence curves were found to be quite complex within the negative delay time range because of the perturbed free-induction decay (PFID) signal [27–29]; therefore, only the temporal dependence curves within the positive time range are plotted in Figure 5. The time-zero point was determined from the ΔOD contour plot in the delay time and wavenumber space because the PFID signal exhibited oscillation behavior at frequencies that were strongly dependent on the probe light wavenumber [the contour plot after time-zero is depicted in Figure 6b with the OD spectra at 100 K (low-*T* insulating phase) and at 200 K (high-*T* metallic phase), for reference in Figure 6a [26,28,29].

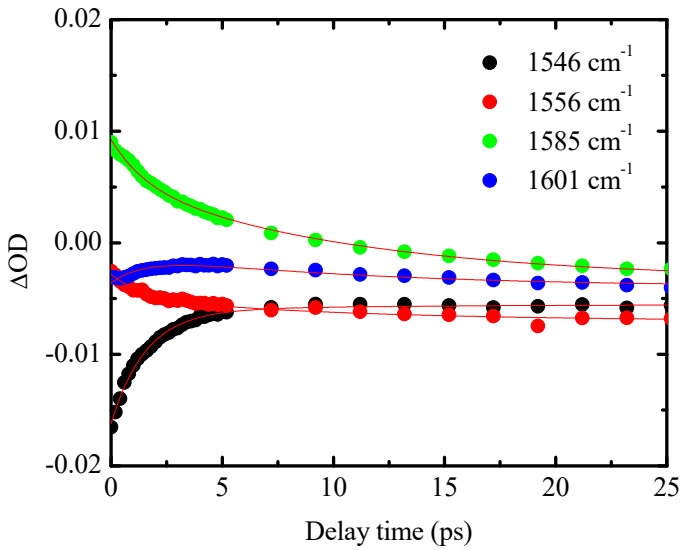

Figure 5. Temporal dependence of the ΔOD value at several wavenumbers in the intramolecular vibration energy range, particularly for the C=C stretching mode of EDO-TTF (or MeEDO-TTF) at 100 K (closed circles). The results of the fitting analysis are also plotted (thin red lines).

Figure 5 illustrates that the absolute values of ΔOD at almost all the wavenumbers show their maximum amplitudes at the time-zero, after which their relaxation behaviors are observed in the positive delay time range. A clear wavenumber dependence is confirmed by the temporal dependence curves observed here; it is thus speculated that the relaxation process may contain multiple processes accompanied by structural changes in the constituent molecules. This speculation is consistent with the

photoinduced dynamics that were probed using the ΔOD value at 0.27 eV, which includes at least three relaxation processes. The existence of these multirelaxation processes is also indicated by the contour plot shown in Figure 6b. For example, the ΔOD at approximately 1585 cm^{-1} was observed to have a longer relaxation time than the ΔOD that occurred around 1615 cm^{-1}. In order to analyze the dataset, we modified Equation (1) slightly based on an energy diagram shown in Figure 7, which assumes serial relaxation processes of the transient states (i), (ii), and (iii). The modified fitting function is:

$$\begin{aligned} f(t) = \quad & A_0(\omega)\exp\left(-\tfrac{t}{\tau_A}\right) + B_0(\omega)\tfrac{\tau_B}{\tau_B-\tau_A}\left\{\exp\left(-\tfrac{t}{\tau_B}\right) - \exp\left(-\tfrac{t}{\tau_A}\right)\right\} \\ & + C_0(\omega)\left\{1 + \tfrac{\tau_A}{\tau_B-\tau_A}\exp\left(-\tfrac{t}{\tau_A}\right) - \tfrac{\tau_B}{\tau_B-\tau_A}\exp\left(-\tfrac{t}{\tau_B}\right)\right\}. \end{aligned} \tag{2}$$

Here, the parameters $A_0(\omega)$, $B_0(\omega)$, and $C_0(\omega)$ are ΔOD of the transient state (i), (ii), and (iii), respectively. $\hbar\omega$ is the photon energy of the probe light. The parameters τ_A and τ_B are relaxation time constants of the transient state (i) and (ii), respectively. A fitting analysis was performed using Equation (2) to determine the photoinduced multirelaxation processes. The fitting curves are also plotted in Figure 5 as red thin lines and well reproduce the experimental results. The fitting analysis shows that the values of τ_A and τ_B are approximately 1.5 ± 0.02 and 11 ± 0.4 ps, respectively. When the error bar and the difference of the excitation intensity are considered, the time scales of these two time constants, τ_A and τ_B, are consistent with the time constants τ_1 and τ_2 that were estimated for the photoinduced dynamics in the electronic structure (see Figure 4). Therefore, it can be concluded that the same photoinduced dynamics are observed using two different probes, i.e., the electronic structure and the intramolecular vibration.

The spectra of the coefficients $A_0(\omega)$, $B_0(\omega)$, and $C_0(\omega)$ are plotted in Figure 6c as black, red, and green closed circles, respectively. Importantly, the spectral shapes of each coefficient represent ΔOD spectra of the transient state and the ground state. The spectral shape of coefficient $A_0(\omega)$ differs considerably from that of any state known as a thermal equilibrium state, as observed during measurement of the T dependence of the OD spectra.

In contrast, the spectral shape of coefficient $B_0(\omega)$ appears to be similar to the difference spectrum of the high-T metallic and low-T insulating phases that are shown in Figure 6d, except for the small difference of the position of the rather broad band located at approximately 1585 cm^{-1}. The observed results strongly indicate that a molecular structure similar to that for the high-T metallic phase appears at approximately 1.5 ps after the fast (τ_A) relaxation process. Note here that the peak position with the positive sign in $B_0(\omega)$, which can be assigned to the C=C stretching mode peak in the transient state, is located at approximately 1585 cm^{-1}. This frequency is slightly higher than that for the thermally induced high-T metallic phase (below 1580 cm^{-1}; see the lower panel of Figure 3c). The observed discrepancies in the intensity and the center frequency of the C=C stretching mode suggest that the excited state that appears approximately 1.5 ps after photoexcitation can also not be assigned to the high-T metallic phase under thermal equilibrium conditions. We, therefore, tentatively assign this state to a unique state under the photoinduced nonequilibrium condition, which is called the nonequilibrium high-T metallic state.

In addition, the spectral shape of coefficient $C_0(\omega)$ appears to be very similar to the difference spectrum of the high-T metallic and low-T insulating phases shown in Figure 6d over the entire observed spectral range. It is, thus, reasonable to propose that the relaxation process is the one from the nonequilibrium high-T metallic state to the equilibrium high-T metallic state. The equilibrium high-T metallic state with relatively long life-time relaxes to the initial low-T insulating phase within 1 ms.

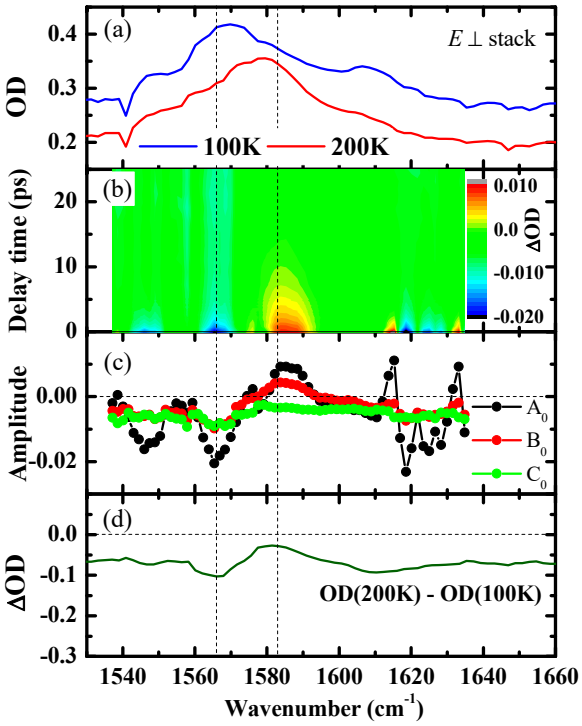

Figure 6. (**a**) OD spectra of the $E \perp$ stack polarization at 200 K ($T > T_C$) and 100 K ($T < T_C$). (**b**) Contour plot of temporal dependence of the ΔOD spectra of the $E \perp$ stack at 100 K. The inset of (**b**) shows the color scale for the ΔOD value. (**c**) Spectra of each component of the fitting function (see text for details). (**d**) Difference spectrum of the OD spectra between the high- (200 K) and low-temperature (100 K) phases.

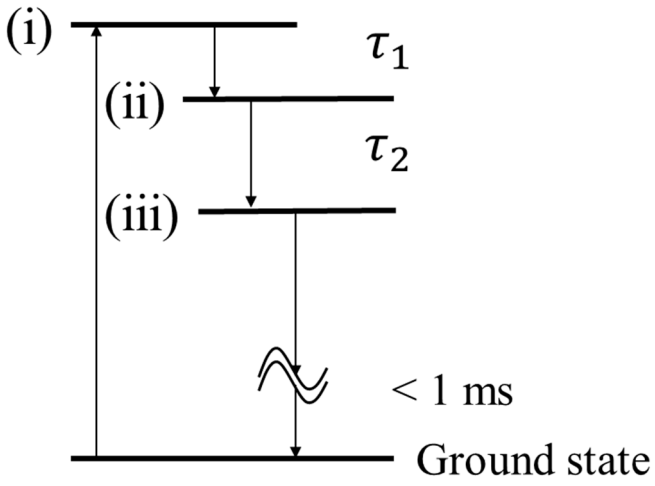

Figure 7. Energy diagram during the photoinduced dynamics in the low-temperature phase proposed from the experimental data. (i), (ii), and (iii) denote the transient states (see text for details).

3.5. Discussion

The photoinduced dynamics observed in the low-T insulating phase of the $[(EDO\text{-}TTF)_{0.89}(MeEDO\text{-}TTF)_{0.11}]_2PF_6$ thin crystal can be understood according to the schematic energy diagram depicted in Figure 7. Immediately after photoexcitation, it is speculated that the optical gap vanishes, as indicated by the ΔOD signal at 0.27 eV shown in Figure 4. Based on the unique spectral shape of component $A_0(\omega)$ in Figure 6, the transient photoinduced state that appears immediately after photoexcitation is the nonequilibrium state that cannot be attributed to any thermal equilibrium state. This transient state (i) seems to be a metallic state, based on the negative value of

ΔOD at 0.27 eV. The transient state (i) relaxes successively to the second (ii) and third (iii) ones with the time constant of approximately 1–1.5 ps and 6–11 ps, respectively. Transient states (ii) and (iii) are tentatively assigned to be a nonequilibrium high-*T* metallic state and an equilibrium high-*T* metallic state, respectively, based on the photoinduced changes in the molecular vibrational spectra discussed with Figure 6. The ΔOD at 0.27 eV at 20 ps is observed to be still showing a negative value; in this case, the time-scale of the recovery of the optical gap observed in the low-*T* insulating phase is much longer than 1 ns. After at least 1 ms, the relaxation processes to the low-*T* insulating phase are completed.

It is also interesting to compare the observed photoinduced dynamics in the insulating phase of the Peierls-type M–I phase transition system with that in pure (EDO-TTF)$_2$PF$_6$. In (EDO-TTF)$_2$PF$_6$, a unique photoinduced state (a hidden state) with a charge pattern of (1010), which differs from the (0110) pattern of the initial low-*T* insulating phase, was indicated to appear as a photoinduced transient state at a very early stage with a time scale of 40 fs [17]. The (1010) CO-type transient insulating state had been observed as a broad reflectivity band that was assigned to a fluctuation of the short range order of (1010) CO and relaxed with a time scale of 50 ps [15]. The high-*T* phase-like metallic state finally appeared at 500 ps [15]. The dynamics observed in [(EDO-TTF)$_{0.89}$(MeEDO-TTF)$_{0.11}$]$_2$PF$_6$ are completely different from that of (EDO-TTF)$_2$PF$_6$ case despite the small difference among them, the anion-donor distance. In [(EDO-TTF)$_{0.89}$(MeEDO-TTF)$_{0.11}$]$_2$PF$_6$, photoexcitation on the low-*T* insulating phase instantaneously extinguishes the optical gap, the state (i), and induces the simultaneous/successive appearances of nonequilibrium, the state (ii), and equilibrium, the state (iii), high-*T* metallic state in the form of transient states. Even the latter state (iii) appears within at least 10 ps after photoexcitation. The time scale required to realize the high-*T* metallic state, regardless of whether it is under nonequilibrium or equilibrium conditions, is clearly shorter in the Peierls-type M–I system than that in pure (EDO-TTF)$_2$PF$_6$. The differences in the time scales of the photoinduced dynamics and the nature of the transient state indicate that the donor-anion interaction, which is introduced by the substitution of EDO-TTF with MeEDO-TTF molecules, is an important factor that governs the photoinduced dynamics.

In future studies, it may be interesting to use a pulsed laser in the mid-IR range with shorter pulse durations to clarify the nature of the photoinduced state (i). In addition, it may also be interesting to measure the spectra of the transient states over a wide energy range and, thus, determine how to collapse and recover the optical gap structure.

Author Contributions: T.I., Y.O., and S.-y.K. conceived and designed the experiments. T.I., Y.O., and K.O. constructed the experimental setup for time-resolved spectroscopy in the electronic transition range. S.T. and K.O. constructed the experimental setup for mid-IR time-resolved vibrational spectroscopy. T.I., Y.U., T.S., and S.T. performed the experiments. T.I. and Y.U. analyzed the data. T.H., Y.N., K.T., and H.Y. contributed materials. T.I. wrote the paper, which reflected discussions with all authors.

Funding: This research was funded by JSPS KAKENHI under grant nos. JP15H02103, JP16K05397, JP17H05153, JP17H06375, JP18H05208, JP18K05260, JP18H05170, and JP26288035. This work was also partially supported by CREST, JST, and PRESTO, JST.

Acknowledgments: We would like to thank the Ookayama Materials Analysis Division for their help in microtoming the single crystals.

Conflicts of Interest: The authors declare no conflict of interest.

References

1. *Photoinduced Phase Transitions*; Nasu, K., Ed.; World Scientific Publishing Co. Pte. Ltd.: Singapore, 2004; ISBN 9789812565723.
2. Yonemitsu, K.; Nasu, K. Theory of Photoinduced Phase Transitions. *J. Phys. Soc. Jpn.* **2006**, *75*, 011008. [CrossRef]
3. Ishiguro, T.; Yamaji, K.; Saito, G. *Organic Superconductors*, 2nd ed.; Springer: Berlin/Heidelberg, Germany, 1998; Volume 88, ISBN 978-3-540-63025-8.
4. Chow, D.S.; Zamborszky, F.; Alavi, B.; Tantillo, D.J.; Baur, A.; Merlic, C.A.; Brown, S.E. Charge ordering in the TMTTF family of molecular conductors. *Phys. Rev. Lett.* **2000**, *85*, 1698–1701. [CrossRef]

5. Clay, R.; Mazumdar, S.; Campbell, D. Pattern of charge ordering in quasi-one-dimensional organic charge-transfer solids. *Phys. Rev. B* **2003**, *67*, 115121. [CrossRef]
6. Kuwabara, M.; Seo, H.; Ogata, M. Coexistence of charge order and spin–peierls lattice distortion in one-dimensional organic conductors. *J. Phys. Soc. Jpn* **2003**, *72*, 225–228. [CrossRef]
7. Clay, R.T.; Ward, A.B.; Gomes, N.; Mazumdar, S. Bond patterns and charge-order amplitude in quarter-filled charge-transfer solids. *Phys. Rev. B* **2017**, *95*, 125114. [CrossRef]
8. Ota, A.; Yamochi, H.; Saito, G. A novel metal-insulator phase transition observed in $(EDO\text{-}TTF)_2PF_6$. *J. Mater. Chem.* **2002**, *12*, 2600–2602. [CrossRef]
9. Drozdova, O.; Yakushi, K.; Yamamoto, K.; Ota, A.; Yamochi, H.; Saito, G.; Tashiro, H.; Tanner, D. Optical characterization of $2k_F$ bond-charge-density wave in quasi-one-dimensional 3/4-filled $(EDO\text{-}TTF)_2X$ (X = PF_6 and AsF_6). *Phys. Rev. B* **2004**, *70*, 075107. [CrossRef]
10. Aoyagi, S.; Kato, K.; Ota, A.; Yamochi, H.; Saito, G.; Suematsu, H.; Sakata, M.; Takata, M. Direct observation of bonding and charge ordering in $(EDO\text{-}TTF)_2PF_6$. *Angew. Chem. Int. Ed.* **2004**, *43*, 3670–3673. [CrossRef] [PubMed]
11. Iwano, K.; Shimoi, Y. Large electric-potential bias in an EDO-TTF tetramer as a major mechanism of charge ordering observed in its PF_6 salt: A density functional theory study. *Phys. Rev. B* **2008**, *77*, 075120. [CrossRef]
12. Tsuchiizu, M.; Suzumura, Y. Peierls ground state and excitations in the electron-lattice correlated system $(EDO\text{-}TTF)_2X$. *Phys. Rev. B* **2008**, *77*, 195128. [CrossRef]
13. Chollet, M.; Guerin, L.; Uchida, N.; Fukaya, S.; Shimoda, H.; Ishikawa, T.; Matsuda, K.; Hasegawa, T.; Ota, A.; Yamochi, H.; et al. Gigantic photoresponse in 1/4-filled-band organic salt $(EDO\text{-}TTF)_2PF_6$. *Science* **2005**, *307*, 86–89. [CrossRef] [PubMed]
14. Onda, K.; Ogihara, S.; Yonemitsu, K.; Maeshima, N.; Ishikawa, T.; Okimoto, Y.; Shao, X.; Nakano, Y.; Yamochi, H.; Saito, G.; et al. Photoinduced change in the charge order pattern in the quarter-filled organic conductor $(EDO{-}TTF)_2PF_6$ with a strong electron-phonon interaction. *Phys. Rev. Lett.* **2008**, *101*, 067403. [CrossRef] [PubMed]
15. Fukazawa, N.; Shimizu, M.; Ishikawa, T.; Okimoto, Y.; Koshihara, S.; Hiramatsu, T.; Nakano, Y.; Yamochi, H.; Saito, G.; Onda, K. Charge and structural dynamics in photoinduced phase transition of $(EDO\text{-}TTF)_2PF_6$ examined by picosecond time-resolved vibrational spectroscopy. *J. Phys. Chem. C* **2012**, *116*, 5892–5899. [CrossRef]
16. Gao, M.; Lu, C.; Jean-Ruel, H.; Liu, L.C.; Marx, A.; Onda, K.; Koshihara, S.-Y.; Nakano, Y.; Shao, X.; Hiramatsu, T.; et al. Mapping molecular motions leading to charge delocalization with ultrabright electrons. *Nature* **2013**, *496*, 343–346. [CrossRef] [PubMed]
17. Matsubara, Y.; Ogihara, S.; Itatani, J.; Maeshima, N.; Yonemitsu, K.; Ishikawa, T.; Okimoto, Y.; Koshihara, S.; Hiramatsu, T.; Nakano, Y.; et al. Coherent dynamics of photoinduced phase formation in a strongly correlated organic crystal. *Phys. Rev. B* **2014**, *89*, 161102. [CrossRef]
18. Onda, K.; Yamochi, H.; Koshihara, S.Y. Diverse photoinduced dynamics in an organic charge-transfer complex having strong electron–Phonon interactions. *Acc. Chem. Res.* **2014**, *47*, 3494–3503. [CrossRef] [PubMed]
19. Servol, M.; Moisan, N.; Collet, E.; Cailleau, H.; Kaszub, W.; Toupet, L.; Boschetto, D.; Ishikawa, T.; Moréac, A.; Koshihara, S.; et al. Local response to light excitation in the charge-ordered phase of $(EDO{-}TTF)_2SbF_6$. *Phys. Rev. B* **2015**, *92*, 024304. [CrossRef]
20. Ishikawa, T.; Kitayama, M.; Chono, A.; Onda, K.; Okimoto, Y.; Koshihara, S.; Nakano, Y.; Yamochi, H.; Morikawa, T.; Shirahata, T.; et al. Probing the metal-insulator phase transition in the $(DMEDO\text{-}EBDT)_2PF_6$ single crystal by optical measurements. *J. Phys. Condens. Matter* **2012**, *24*, 195501. [CrossRef]
21. Liu, L.C.; Jiang, Y.; Mueller-Werkmeister, H.M.; Lu, C.; Moriena, G.; Ishikawa, M.; Nakano, Y.; Yamochi, H.; Miller, R.J.D. Ultrafast electron diffraction study of single-crystal $(EDO\text{-}TTF)_2SbF_6$: Counterion effect and dimensionality reduction. *Chem. Phys. Lett.* **2017**, *683*, 160–165. [CrossRef]
22. Murata, T.; Shao, X.; Nakano, Y.; Yamochi, H.; Uruichi, M.; Yakushi, K.; Saito, G.; Tanaka, K. Tuning of multi-instabilities in organic alloy, $[(EDO\text{-}TTF)_{1-x}(MeEDO\text{-}TTF)_x]_2PF_6$. *Chem. Mater.* **2010**, *22*, 3121–3132. [CrossRef]
23. Hiramatsu, T.; Murata, T.; Shao, X.; Nakano, Y.; Yamochi, H.; Uruichi, M.; Yakushi, K.; Tanaka, K. Phase transition behavior in the mixed crystal of pristine and mono-methyl substituted EDO-TTF. *Phys. Status Solidi (C)* **2012**, *9*, 1155–1157. [CrossRef]

24. Fukazawa, N.; Tanaka, T.; Ishikawa, T.; Okimoto, Y.; Koshihara, S.; Yamamoto, T.; Tamura, M.; Kato, R.; Onda, K. Time-resolved infrared vibrational spectroscopy of the photoinduced phase transition of $Pd(dmit)_2$ salts having different orders of phase transition. *J. Phys. Chem. C* **2013**, *117*, 13187–13196. [CrossRef]
25. Matsubara, Y.; Okimoto, Y.; Yoshida, T.; Ishikawa, T.; Koshihara, S.; Onda, K. Photoinduced neutral-to-ionic phase transition in tetrathiafulvalene-p-chloranil studied by time-resolved vibrational spectroscopy. *J. Phys. Soc. Jpn.* **2011**, *80*, 124711. [CrossRef]
26. Ishikawa, T.; Hosoda, R.; Okimoto, Y.; Tanaka, S.; Onda, K.; Koshihara, S.; Kumai, R. Direct observations of the photoinduced change in dimerization in K-TCNQ. *Phys. Rev. B* **2016**, *93*, 195130. [CrossRef]
27. Joffre, M.; Hulin, D.; Migus, A.; Antonetti, A.; Benoit à la Guillaume, C.; Peyghambarian, N.; Lindberg, M.; Koch, S.W. Coherent effects in pump-probe spectroscopy of excitons. *Opt. Lett.* **1988**, *13*, 276–278. [CrossRef]
28. Hamm, P. Coherent effects in femtosecond infrared spectroscopy. *Chem. Phys.* **1995**, *200*, 415–429. [CrossRef]
29. Yan, S.; Seidel, M.T.; Tan, H.-S. Perturbed free induction decay in ultrafast mid-IR pump–probe spectroscopy. *Chem. Phys. Lett.* **2011**, *517*, 36–40. [CrossRef]